Earth Syst. Sci. Data, 6, 185–200, 2014
www.earth-syst-sci-data.net/6/185/2014/
doi:10.5194/essd-6-185-2014


Open Access Earth System Science Data

# A global radiosonde and tracked balloon archive on 16 pressure levels (GRASP) back to 1905 – Part 1: Merging and interpolation to 00:00 and 12:00 GMT

**L. Ramella Pralungo[1], L. Haimberger[1], A. Stickler[2,3], and S. Brönnimann[1]**

[1]Department of Meteorology and Geophysics, University of Vienna, Althanstrasse 14, 1090 Vienna, Austria
[2]Oeschger Centre for Climate Change Research, Bern, Switzerland
[3]Institute of Geography, University of Bern, Switzerland

*Correspondence to:* L. Ramella Pralungo (lorenzo.ramella-pralungo@univie.ac.at)

Received: 5 December 2013 – Published in Earth Syst. Sci. Data Discuss.: 23 December 2013
Revised: 7 April 2014 – Accepted: 12 April 2014 – Published: 22 May 2014

**Abstract.** Many observed time series of the global radiosonde or PILOT networks exist as fragments distributed over different archives. Identifying and merging these fragments can enhance their value for studies on the three-dimensional spatial structure of climate change.

The Comprehensive Historical Upper-Air Network (CHUAN version 1.7), which was substantially extended in 2013, and the Integrated Global Radiosonde Archive (IGRA) are the most important collections of upper-air measurements taken before 1958. CHUAN (tracked) balloon data start in 1900, with higher numbers from the late 1920s onward, whereas IGRA data start in 1937. However, a substantial fraction of those measurements have not been taken at synoptic times (preferably 00:00 or 12:00 GMT) and on altitude levels instead of standard pressure levels. To make them comparable with more recent data, the records have been brought to synoptic times and standard pressure levels using state-of-the-art interpolation techniques, employing geopotential information from the National Oceanic and Atmospheric Administration (NOAA) 20th Century Reanalysis (NOAA 20CR). From 1958 onward the European Re-Analysis archives (ERA-40 and ERA-Interim) available at the European Centre for Medium-Range Weather Forecasts (ECMWF) are the main data sources. These are easier to use, but pilot data still have to be interpolated to standard pressure levels.

Fractions of the same records distributed over different archives have been merged, if necessary, taking care that the data remain traceable back to their original sources. If possible, station IDs assigned by the World Meteorological Organization (WMO) have been allocated to the station records. For some records which have never been identified by a WMO ID, a local ID above 100 000 has been assigned. The merged data set contains 37 wind records longer than 70 years and 139 temperature records longer than 60 years. It can be seen as a useful basis for further data processing steps, most notably homogenization and gridding, after which it should be a valuable resource for climatological studies.

Homogeneity adjustments for wind using the NOAA-20CR as a reference are described in Ramella Pralungo and Haimberger (2014). Reliable homogeneity adjustments for temperature beyond 1958 using a surface-data-only reanalysis such as NOAA-20CR as a reference have yet to be created.

All the archives and metadata files are available in ASCII and netCDF format in the *PANGAEA* archive doi:10.1594/PANGAEA.823617.



Published by Copernicus Publications.

## 1 Introduction

The radiosonde and pilot balloon network was practically the only global upper-air observing system up to the late 1970s and is still a valuable source of meteorological and climatological information, although there are now plenty of other observations such as satellite or aircraft data (Dee et al., 2011). While several global radiosonde archives exist and are publicly available, such as the Integrated Global Radiosonde Archive (Durre et al., 2006) or CHUAN (Stickler et al., 2010, 2014), they only partly fulfil the needs of climate scientists due to inhomogeneities in the data and since wind data from tracked balloons are often not available on standard pressure levels.

Almost all homogenized radiosonde data sets published so far, most notably Radiosonde Atmospheric Temperature Products for Assessing Climate (RATPAC) (Free et al., 2005), manually and automatically homogenized versions of the Hadley Centre Atmospheric Temperature (HadAT) (Thorne et al., 2005, 2011), Iterative Universal Kriging (IUK) (Sherwood et al., 2008) as well as Radiosonde Observation Correction using Reanalyses (RAOBCORE) (Haimberger, 2007; Gruber and Haimberger, 2008) and Radiosonde Innovation Composite Homogenization (RICH) (Haimberger et al., 2012), only go back to 1958 since radiosonde and pilot launch times had not been standardized to synoptic times (mostly 00:00 and 12:00 GMT). While radiosonde data are reported on significant pressure levels (levels where the vertical temperature gradient changes) and often have been interpolated to standard pressure levels (10, 20, 30, 50, 70, 100, 150, 200, 250, 300, 400, 500, 700, 850, 1000 hPa), wind data from tracked balloons are mostly given on altitude levels. These altitude levels are relative to the sea level. Without additional temperature information at least every 12 h, it is not possible to interpolate those wind data to standard pressure levels accurately enough to make them suitable for climate analysis.

Not surprisingly there are very few upper-air wind climatologies so far that go back beyond 1958, and most of them work with monthly data although thousands of ascents are available back to the 1920s. Some studies have analysed the flow fields during special climatological events such as the Dust Bowl drought in the 1930s (Brönnimann et al., 2009). In a pioneering study, Brönnimann and Luterbacher (2004) used the data presented in "A historical upper air-data set for the 1939–1944 period" (Brönnimann, 2003) to characterize climate anomalies in troposphere and stratosphere in association with the particularly strong El Niño event of 1940–1942. Grant et al. (2009) studied low-frequency variability and trends of upper-air temperature and geopotential but not winds.

The present study intends to improve the data availability by providing temperature and wind time series as far back as such data exist, but only on standard pressure levels. Data on altitude levels are interpolated to standard pressure levels using temperature information from the NOAA Twentieth Century Reanalysis (20CR) (Compo et al., 2011). It is required that the time series are from ascending balloons (not kites or tethered balloons) and are at least 300 days long. As such the data set is smaller than CHUAN (Stickler et al., 2014) but is easier to use for time-series analysis. The source data sets are described in the next section. Details on the interpolation methods to standard time/pressure are given in Sect. 3, and data counts and some results are presented in Sect. 4.

## 2 Input data

Creating a uniform radiosonde data set is challenging. There exist many different data sources, and various digitization efforts around the globe have yielded valuable data, but in different formats. However, one can build on the results of earlier integration efforts. These are

- the Comprehensive Historical Upper-Air Network (CHUAN) data set version 1.7 (Stickler et al., 2010; Wartenburger et al., 2013) and the ERA-CLIM Historical Upper-Air Data (Stickler et al., 2014). The ERA-CLIM historical upper-air data set (termed ECUD here) contains upper-air data collected and digitized within the EU 7th Framework Programme project ERA-CLIM. These archives contain mainly historical upper-air data prior to the International Geophysical Year 1957. The data sets consist of 20 million balloon measurement values in around 5000 files that represent ca. 2000 stations with geopotential, temperature, wind and humidity data. The first record goes back to 1900. Those data, as well as some post 1957 data, have never been actively assimilated.

- the Integrated Global Radiosonde Archive (IGRA) (Durre et al., 2006), updated until 2012. IGRA contains data on standard and significant pressure levels and, sometimes, complementary altitude levels (not used in this work, since they do not add information to the pressure data). It is quite comprehensive and goes back to 1938. However, this data set has its geographical focus on America and lacks a lot of data over Europe prior to the mid-1960s.

- the ERA-40 observation input data set. This data set in BUFR format has lots of overlap with IGRA but contains additional data over Europe, Japan and Antarctica that are missing in IGRA. The ERA-40 data set starts in late 1957 and ends in 2002, however only data from 1958–1978 are used.

- the ERA-Interim observation input data set (Dee et al., 2011). It is equivalent with ERA-40 observation input from 1979 to 2012 but is available in the far more convenient ODB format. The ERA-Interim input data set goes

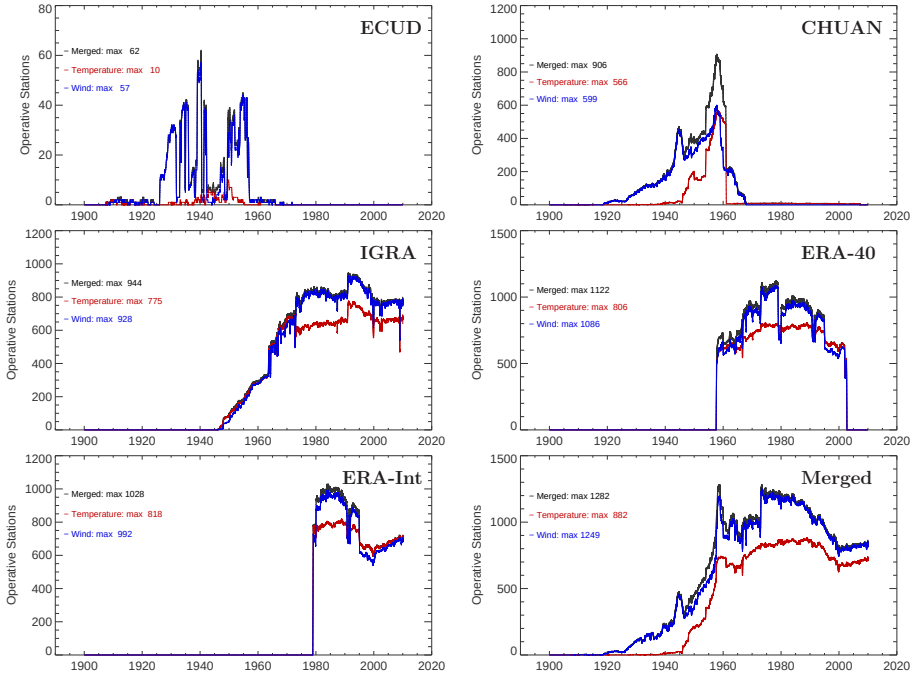


**Figure 1.** Time series of the numbers of active stations from the respective archives considered in this study. Only data from those stations are counted that have at least 365 ascents. The bottom right picture is the merged archive.

up to present and is preferred to ERA-40 from 1979 onward.

– the NOAA 20th century reanalysis (Compo et al., 2011). It does not contain radiosonde information but its geopotential field can be used to calculate pressure information for altitude levels. Since it is available back to 1871, even the earliest upper-air data can be brought to pressure levels. In this work, it has been used as auxiliary data set for time/pressure interpolation and for quality control purposes.

Not only the observation input data are used from the reanalysis data sets. Analyses and background forecasts from ERA-40, ERA-Interim and the NOAA 20th century reanalysis archives all provide valuable reference fields for comparison with radiosonde/pilot data. Observation minus analysis departures (obs – an) from the NOAA-20CR have been calculated for all observations used. In addition observation minus background departures (obs – bg) have been extracted for both ERA-40 and ERA-Interim back to 1958. These are an integral part of the data set prepared here, and they can greatly facilitate homogenization efforts as has been demonstrated by Haimberger (2007); Haimberger et al. (2008); Gruber and Haimberger (2008); Haimberger et al. (2012).

Figure 1 shows the number of records as function of time in the different archives. While the data count in ECUD and CHUAN prior to 1958 is small compared to the period after 1958, the information content of these archives is very high since practically no other upper-air information is available at this time. Figures 2 and 10 show also the spatial extent of the data sets. ECUD contains some very valuable early data at remote places such as northern Russia and India, and the data count will soon increase in the future since several not yet digitized upper-air data have recently been identified and will be digitized in ongoing efforts (Allan et al., 2011; Jourdain and Roucaute, 2013).

Our next step is now to merge all those archives to get long time series, spanning the whole operative time of all the available stations.

## 3 Station identification

The station identification procedure is crucial in order to be able to join different records coming from the same station but stored in different archives. For data assimilated in ERA-40 or ERA-Interim, this is relatively straightforward since the data must have World Meteorological Organization (WMO) number and precise coordinates (latitude, longitude, altitude and time) in order to be assimilated. The IGRA offers WMO ID numbers and coordinates for all its station records as well. The situation is much more difficult for CHUAN and ECUD archives where only around 42 % of the station records have a WMO ID and 74 % have at least a WMO and/or Weather Bureau Army Navy (WBAN) ID number. It has been recognized that many of the unknown station records can be related to WMO ID numbers because of the available geographical information. Nevertheless automatic methods to

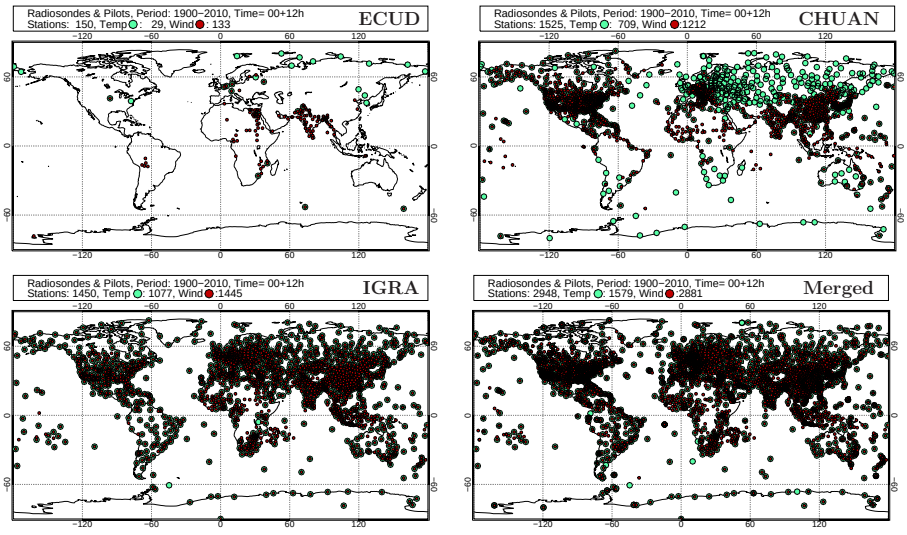


**Figure 2.** Spatial distributions of stations with at least 365 days of data, at the pressure levels of 850, 700 and 500 hPa, in the different data sets used in this study. The bottom right panel shows the distribution in the merged archive. Only WMO stations have been used.

assign the correct WMO numbers to these stations are complex, if not impossible, for the following reasons:

- the station names differ in different archives, and sometimes they are reported in local language including non-standard ASCII characters.
- In many cases the station ID was changed even when the station was relocated only by a few kilometres, which ended the old record and started a new one. In those cases it is possible to join those records without introducing inhomogeneities.
- In other cases different stations were operative simultaneously (pilot at daytime and radiosonde at nighttime, for instance) in the same area/city; even if they are close to each other, they should be identified as independent stations at first since the data have to be processed differently. Only after the pilot data have been brought from altitude levels to standard pressure levels, merging is possible.
- Cases of erroneous coordinates (typos, exchanged signs etc.) were detected.
- While CHUAN also contains some aircraft, kite and tethered balloon data, these have not been included in the merged data set because of their different characteristics (staying at the same height, often for hours) compared to ascending balloons.

The following four station metadata files (they can be downloaded from doi:10.1594/PANGAEA.823609) have been consulted to manually identify the station records:

- WMO Observing Stations and WMO Catalogue of Radiosondes
- radiosonde comprehensive metadata catalogue (Texas University)
- ERA40 radiosonde list with metadata events
- NOAA WBAN and WMO collection.

Since none of the above metadata file is complete, all of them are essential to assign and validate stations WMO ID numbers. If the lat/long information in the four listed station inventory files were incoherent, a manual check via Google Maps was made, and the wrong entries were discarded. In most cases the most recent station location was trusted. If WMO ID number and lat/long were perfectly matching (most of the cases), the station identification was straightforward. When the station name was the same (considering the different languages and typos) and lat/long were almost (within $< 0.5°$) but not perfectly matching, the station location was monitored with Google Maps. In the majority of cases, a relocation of the station within the same area/city (e.g. from university to airport, from an airport to another) was the reason, and the most recent WMO ID was kept. Stations with implausible lat/long (wrong sign, inverted digits) were highlighted, and, after a double check (if possible), their metadata were corrected. Where the localization was unsafe, no WMO ID number was assigned. As a result of those efforts, roughly 95 % of the CHUAN stations could be identified with a WMO ID number. Nevertheless, the stations not identified were analysed and stored if their records were long enough. A table with station identifiers (file station_list.txt) is presented in the supplements section of the PANGAEA website. Where the latitude and/or the longitude are missing or are unrealistic in the station list inventory, the station was rejected.

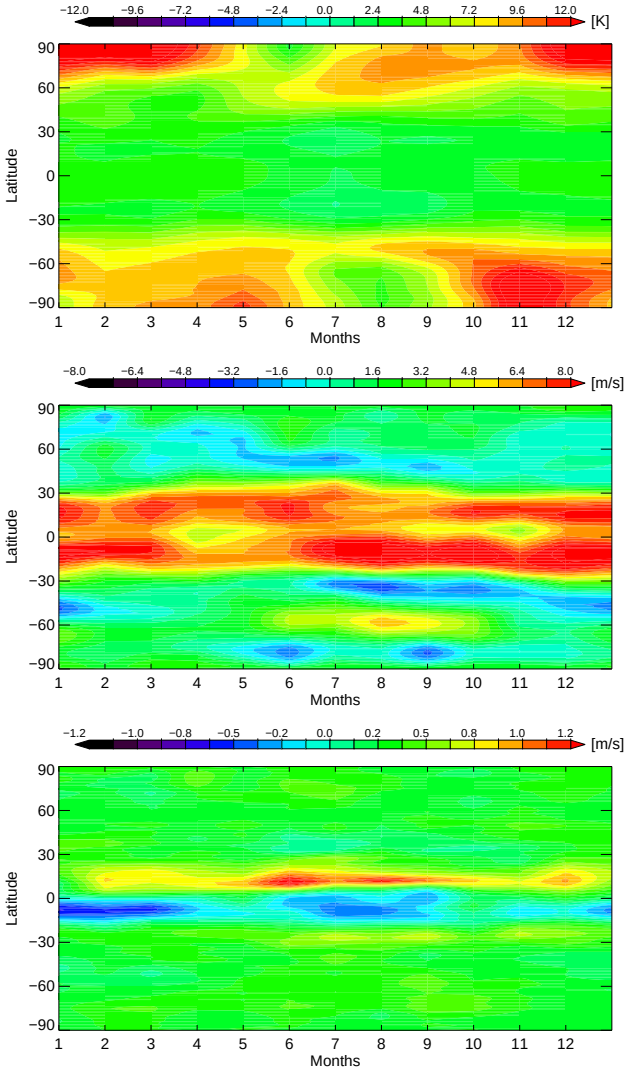


**Figure 3.** Zonal mean temperature (top), $U$ (middle) and $V$ (bottom) wind biases of NOAA-20CR compared to ERA-Interim at 150 hPa averaged over 00:00 and 12:00 UTC and over each month of the year 1979. Note different scales for $U$ and $V$ components.

## 4 Interpolation from altitude to standard pressure levels

The pilot balloons used for upper-air wind measurements were tracked using theodolites or RADAR. Both instruments report geometrical height as vertical coordinate. In both CHUAN and ECUD, the wind observations are reported on altitude levels (m a.s.l.). An accurate interpolation from altitude to pressure (most likely not standard) and, in a second step, from non-standard pressure to standard pressure levels requires either temperature plus humidity or geopotential information. Using standard atmosphere temperature values would introduce unnecessarily large errors.

Geopotential information is available globally every 6 h on a $2^\circ \times 2^\circ$ grid from the NOAA 20CR. These are interpolated bilinearly to the respective station locations (latitude/longitude). While the NOAA 20CR analysis fields are means of an ensemble, and thus spatially relatively smooth, they represent a substantial improvement compared to climatological fields or the standard atmosphere. There are some biases of temperature (and thus geopotential) fields at high tropospheric/low stratospheric levels especially in the polar regions (see Fig. 3a). However, they introduce a small bias, especially before the 1950s since only few ascents reached levels higher than 500 hPa. This can be seen also from Fig. 5.

At the station location we can now find the interpolation weight $a$ from the formula

$$\phi_x = a \cdot \phi_1 + (1 - a) \cdot \phi_2, \quad (1)$$

where $\phi_1 < \phi_x < \phi_2$, where $\phi_1$ and $\phi_2$ are geopotential values at NOAA-20CR model levels at the station location and $\phi_x$ is the reported altitude of the measurement multiplied by $g$. Now it is possible to determine the corresponding pressure at the station location $p_x$ as $\ln p_x = a \cdot \ln p(\phi_2) + (1 - a) \cdot \ln p(\phi_1)$. In order to obtain values on standard pressure levels, we perform again a linear interpolation from pressure $\phi_x$ levels to standard levels. The latter procedure is necessary also for assimilated pilot (from ERA-40 and ERA-Interim input data) since those are only available on significant levels but not standard levels.

## 5 Time interpolation

Not all radiosonde and pilot stations report at 00:00 and 12:00 GMT. Particularly before 1958 the launch times were not standardized. In order not to discard too many observations at asynoptic times, also a time interpolation has been implemented that allows backwards continuation of many records. To take into account the diurnal cycle in the temperature and wind fields, we assume that the difference between observation and the reference NOAA 20CR is constant within $\pm 6$ h of the observations. This assumption is justifiable for wind, since wind measurement biases as well as NOAA 20CR biases are not expected to depend strongly on the observation hour, at least not in the vertical mean. The analysis value at the time of the observation $t_{\mathrm{obs}}$ is gained by cubic interpolation. Then it is assumed that the analysis departure at time $t_{\mathrm{obs}}$ is still (already) valid at 00:00 or 12:00 GMT.

The observations are divided in three time categories as outlined in Table 1. The time offset is at most 6 h, which is crude. It could, in principle, be reduced to 3 h if four synoptic times per day were considered instead of just two. Using the departure definition,

$$\tau(t_{\mathrm{obs}}) = \mathrm{obs}(t_{\mathrm{obs}}) - \mathrm{20CR}(t_{\mathrm{obs}}), \quad (2)$$

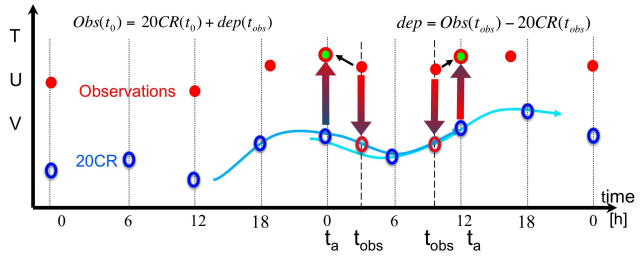


**Figure 4.** Time interpolation. When there are no observations available at 00:00 or 12:00 UTC but only at other times, a reference value at the time of the asynoptic observation $t_{obs}$ is calculated from the NOAA 20CR, employing a cubic interpolation with the four closest values. The difference $dep(t_{obs}) = Obs(t_{obs}) - 20CR(t_{Obs})$ is assumed constant between $t_{obs}$ and the closest synoptic time $t_a$. The observation at time $t_a$ is obtained by adding the departure $dep(t_{obs})$ to $20CR(t_a)$.

**Table 1.** Assignment strategy for observations for interpolation to the nearest synoptic time.

| Observation | Closest synoptic time |
|---|---|
| $<$ 06:00 UTC | 00:00 UTC |
| $\geq$ 06:00 UTC and $\leq$ 18:00 UTC | 12:00 UTC |
| $>$ 18:00 UTC | 00:00 UTC (day after) |

we estimate the observation at the synoptic time 00:00 and 12:00 UTC as

$$\begin{aligned} \mathrm{obs}(t_0) &= 20\mathrm{CR}(t_0) + \tau(t_{\mathrm{obs}}), \\ \mathrm{obs}(t_{12}) &= 20\mathrm{CR}(t_{12}) + \tau(t_{\mathrm{obs}}). \end{aligned} \quad (3)$$

Figure 4 summarizes the idea: the first two observations at synoptic time have not been manipulated. The third one has been reported at 03:00 UTC, and we would like to shift it to 00:00 UTC. For this purpose we interpolate cubically, using the four closest analysis data, the NOAA 20CR (it could be temperature or $U$ or $V$ wind component) to the observation time, and we calculate the departure observation minus reference. In a second step, we add the departure to the NOAA 20CR value at 00:00 UTC (in this case, $t_a$ in the picture), obtaining the reconstructed observation at the standard time 00:00 UTC. We take care that the same observation is not duplicated at 00:00 and 12:00 UTC.

While the time interpolation method may be sufficient for wind, it is certainly problematic for temperature. The diurnal cycle of the NOAA-20CR temperatures may not always be realistic and the temperature measurement biases of the early radiosondes can be large and can change quickly with local time, particularly at dawn or dusk (Nash and Schmidlin, 1987; Andrae et al., 2004; Redder et al., 2004). In order to facilitate the implementation of an improved interpolation or homogenization procedure that may be able to take into account these sharp transitions, the merged data set contains not only the (new) standardized launch times but also the original launch times.

The quality of the interpolation procedure can be assessed by comparing the interpolated values from the CHUAN archive with data from the same stations in the ERA-40 archive, which has been possible at least for the years 1957/58. ERA-40 used "first guess at appropriate time" (Uppala et al., 2005), meaning that the background was compared to an observation at the time of the observation and not at the nearest synoptic time. Also the analysis and background forecast quality was higher because upper-air data were assimilated. Nevertheless, the mean difference between temperatures interpolated to standard pressure levels is very small (rms difference less than 0.1 K), as expected, since the source data should be the same in CHUAN and ERA-40. There is only a vertically constant difference of 0.05 K (not shown), which is likely attributable to a different conversion from °C to K. In this work, the constant 273.15 has been employed.

## 6 Merging the different archives

The good agreement between the time series stemming from ECUD, CHUAN, IGRA, ERA-40 and ERA-Interim suggests that it is generally safe to merge these archives into a global one, in order to get longer, more complete and usable time series.

Figure 1 shows the temporal development of the upper-air temperature and wind station numbers in the different archives. While systematic wind observations begin in the 1920s (data stored in the ECUD and CHUAN archives), the systematic upper-air temperature observations start only after 1940 (CHUAN and IGRA). The ECUD record of Meteorologisches Observatorium Lindenberg/Richard-Aßmann Observatorium (ID 10393) in Germany, where also the GRUAN (Seidel et al., 2009) lead centre is located, holds the earliest data with the first ascent dated 4 April 1900. Regular ascents, started in 1905, making the Lindenberg series the longest, continuous upper-air series in the world (Adam and Dier, 2005).

In order to merge all the stations and to ensure efficiency, the following rules have been adopted:

- Station WMO ID must be the same.
- Station location (latitude, longitude and altitude) must be the same (with $\pm 0.5°$ tolerance) in the source archives.
- A data priority has been set: (1) ERA-Interim, (2) ERA-40, (3) IGRA, (4) CHUAN and (5) ECUD. This means the following: if ERA-Interim data were available, they were used except for those found erroneous in the quality control step outlined below. Then, ERA-40 was used to fill the gaps left by ERA-Interim, then IGRA, then CHUAN and finally ECUD. Thus the ECUD data are

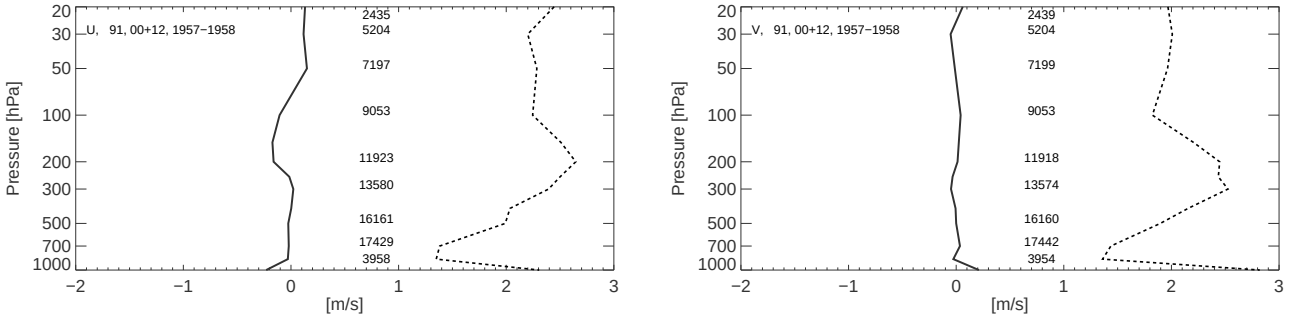


**Figure 5.** Mean (solid) and rms (dashed) $U$ (left panel) and $V$ (right panel) difference between observations interpolated to standard pressure levels in CHUAN and ERA-40, averaged over 91 stations at 00:00 and 12:00 UTC, for the period 1957–1958 in North America. The total number of observations at each pressure level is also reported. Differences come mostly from different temperatures used for interpolation to pressure levels. Only WMO stations have been used.

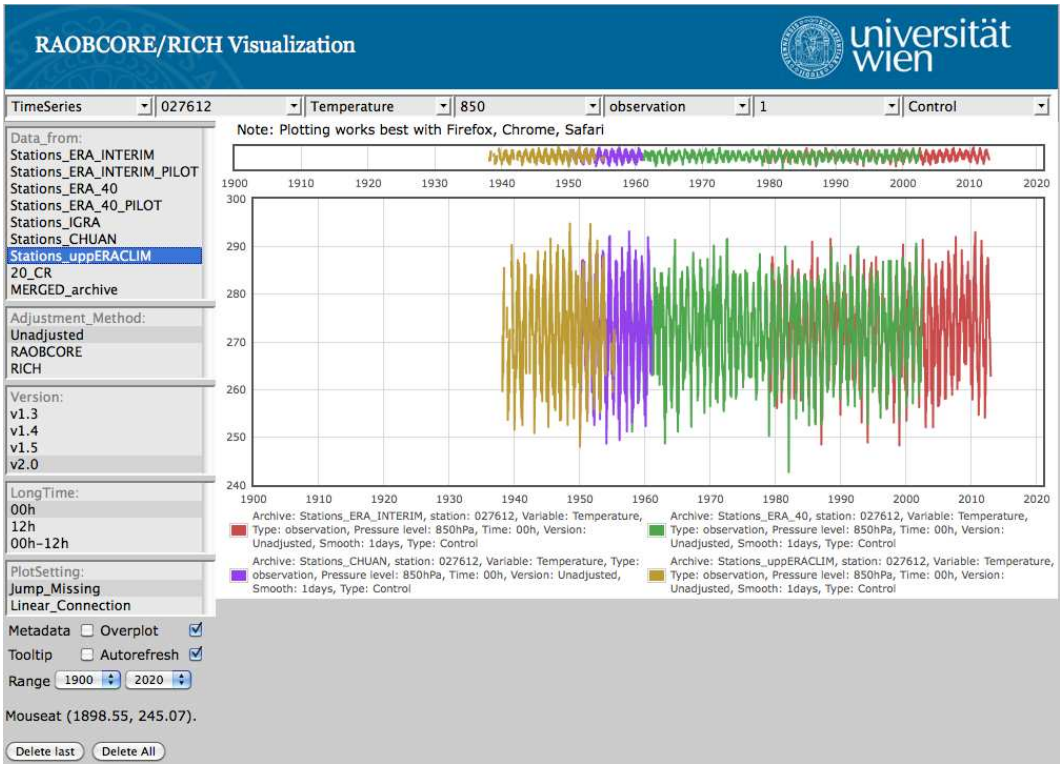


**Figure 6.** Observed temperature time series at station Moscow (027612, Russia) at 850 hPa, at 00:00 UTC. The plot shows the longest and complete temperature time series in the merged archive (1938–2012): red is ERA-Interim, green ERA-40, violet CHUAN and yellow ECUD. The imperfect overlap between the common parts of the archives is a JavaScript artifact which applies a smoothing function if the number of points exceeds the plot resolution. If one zooms in with the time-series viewer, the discrepancies vanish.

used only if they were found in none of the above data sets. The merge procedure is done for every measurement; that is a record for a particular day can consist of values from different archives.

– After the merger, only merged stations with more than 365 days have been kept.

The time series of Moscow in Fig. 6 is an example of a time series that has unique contributions from each of the data sets. It is also one of the very few stations that have temperature data before 1940. One can see the overlap between data sets. The data in the plot do not exactly overlap because the time series are individually sampled, and not the same days are picked for the different data sets.

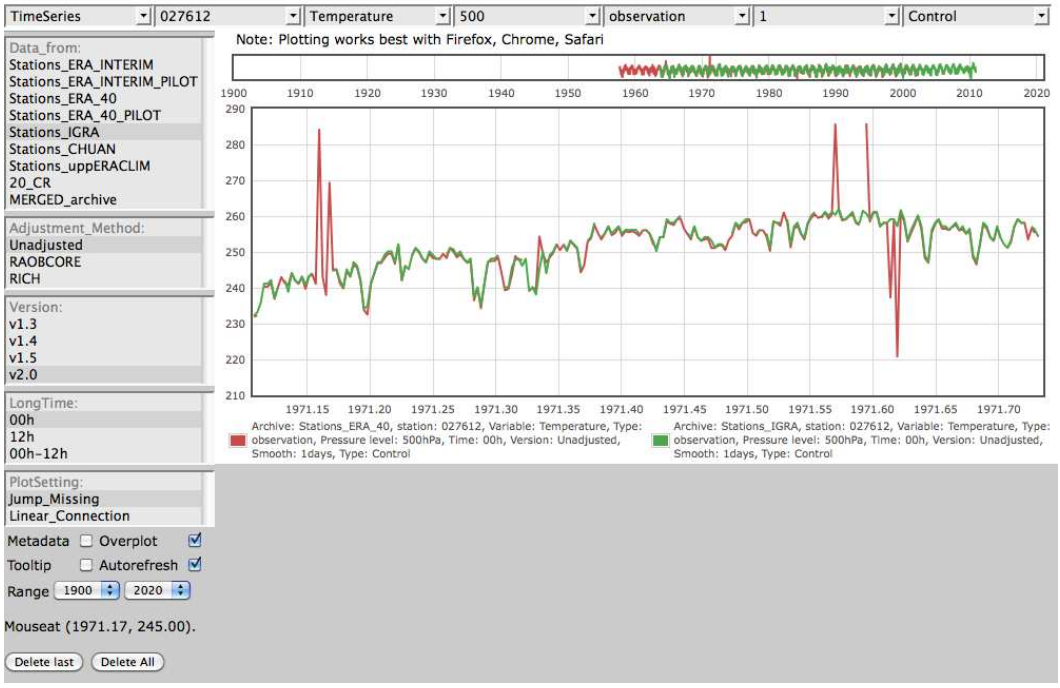


**Figure 7.** Temperature observation time series of station Moscow at 500 hPa and at 00:00 UTC green curve IGRA archive, red curve ERA-40 station archive. The early spikes show a case where no data are available in the IGRA archive and where the data in the ERA-40 are suspicious. The later spikes are caused by four suspicious values reported by the ERA-40 archive. The IGRA archive contains more plausible values on these days.

The $U$ and $V$ wind components over the US also show good agreement between CHUAN and ERA-40 (Fig. 5). The shown differences originate from the different adopted methods for the conversion of altitude to standard pressure levels. The biases are negligible; the largest rms departures are located around 300 and 150 hPa, where there are large vertical wind gradients and the known temperature biases in the NOAA 20CR reanalysis may also lead to geopotential biases that affect the interpolation quality. One also has to bear in mind that the NOAA-20CR analysis fields are estimated to be as accurate as modern 4-day forecasts (Compo et al., 2011). Thus variability due to uncertainty in the analyses also adds to the found rms departures. Newer surface-data-only reanalyses such as ERA-20C (Poli et al., 2013) or the planned Sparse Input Reanalysis for Climate Applications (SIRCA, Compo et al., 2012) are expected to have smaller temperature biases, which should further improve the interpolation quality for both temperature and wind.

For each observed value at day $i$ (a day) at station $j$ for parameter $\phi$ (temperature, wind) denoted as ${}^{i}\mathrm{obs}_{\phi}^{j}$, there also exists an interpolated analysis value ${}^{i}20\mathrm{CR}_{\phi}^{j}$ from the NOAA-20CR. The analysis departures from the NOAA 20CR can thus be written as

$$ {}^{i}\tau_{\phi}^{j} = {}^{i}\,\mathrm{obs}_{\phi}^{j} - {}^{i}\,20\mathrm{CR}_{\phi}^{j}. \quad (4) $$

A simple quality control has been performed on the raw data:

- Date and time limits must be plausible ($00{:}00 < \mathrm{time} < 23{:}59$; we assume $24{:}00 = 00{:}00$ of the next day, Gregorian calendar).
- Temperature must be between $-100$ and $+60\,^{\circ}\mathrm{C}$ or the equivalent in K.
- Wind speed must be between 0 and $200\,\mathrm{m\,s^{-1}}$.
- Wind direction must be between 0 and 360°.

Inside those ranges, the observations may still contain very unlikely/wrong values due to many possible causes, the most likely being typos in the log books and digitization mistakes. The observation was dropped during the merging procedure if its analysis departure ${}^{i}\tau_{\phi}^{j}$ was larger than 4 times the standard deviation $\sigma$ of the departures for the considered pressure level. Before this criterion was applied, the NOAA-20CR was adjusted for its climatological biases, which are strongest in polar regions (see Brönnimann et al., 2012, but can be found also at some locations in the tropics (Stickler and Brönnimann, 2011).

These have been quantified from mean differences between the NOAA-20CR and ERA-Interim in the year 1979. ERA-Interim is considered as one of the most reliable reanalyses (Blunden and Arndt, 2013). Figure 3 shows as an example the global temperature, $U$ and $V$ wind component difference ERA-Interim minus NOAA-20CR at 150 hPa, averaged over 00:00 and 12:00 UTC, for the year 1979. There is

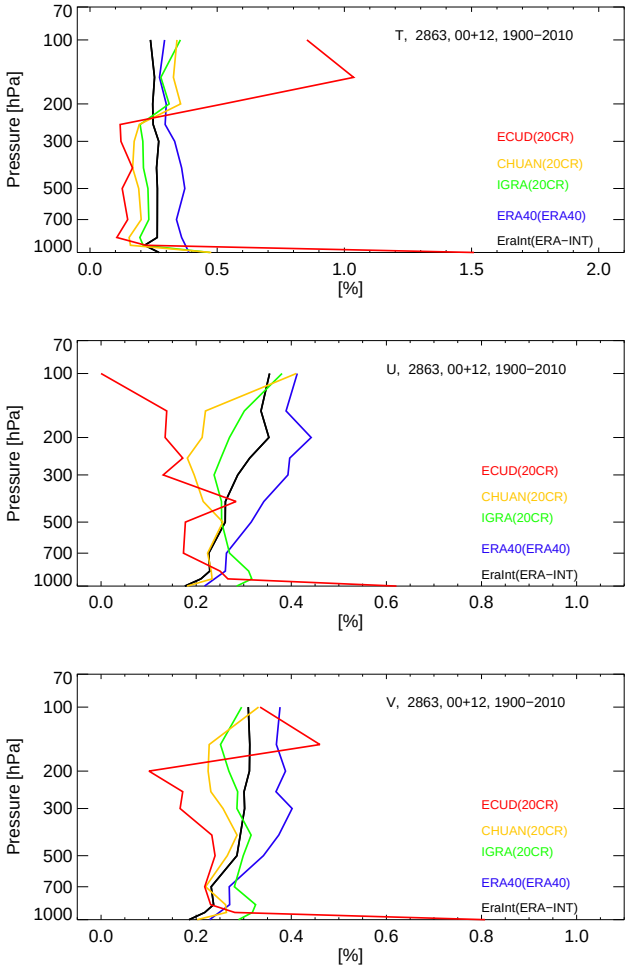


**Figure 8.** Temperature (upper panels) and $U$ (middle panels) and $V$ (bottom panels) wind component spike frequency (%) as function of pressure, for the whole period 1900–2010. The legend contains the archive names and the departure types (in brackets). Values with deviations larger than $4\sigma$ from the respective background forecasts or analyses are counted as spikes.

a warm bias at high latitudes (beyond 60° N and 60° S, reaching up to 12 K), which also has a strong annual cycle. The strongest biases in the $U$ wind component (up to 8 m s$^{-1}$) are concentrated in the tropical regions, with only a weak annual cycle. The zonal mean $V$ wind component, which is small anyway, does not show strong biases. NOAA-20CR temperatures have been shifted by the difference between ERA-Interim and NOAA-20CR. NOAA-20CR wind components have been scaled to match those in ERA-Interim.

Figure 7 highlights the presence of spikes in the raw time series of some archives. Those erroneous values are not propagated to the merged archive. Results of a more comprehensive spike evaluation can be found in Fig. 8, showing that almost all archives exhibit spike densities below 0.5 % for all pressure levels. An exception is ECUD for temperature at 150 hPa: there, the spike rate is 1 %. The ECUD temperature measurements were made prior to 1957 and mostly stem from Siberia. Their special location may explain the different frequency of spikes at high levels. Spikes in the wind time series are relatively rare.

## 7 The merged archived

The union of all data sets gives a total of 3217 stations (land stations and anchored weather ships that use radiosondes, tracked balloons, with time series longer than 365 days), where 3020 have been recognized as WMO stations with a valid WMO ID. A total of 1598 (1596 with WMO ID) stations contain temperature observations, and 3152 (2957 with WMO ID) stations contain wind observations (as $U$ and $V$ components). The Lindenberg (WMO ID 10393) series starts already in 1900, but it contains several gaps. The longest continuous upper-air temperature record comes from Moscow with data available from 1938 onward.

Figure 9 shows three temperature departure time series at 500 hPa for Moscow (WMO ID 26712, Russia). The longest series (observation minus NOAA-20CR analysis) goes as far back as the observations. Of course it already shows much smaller variance than the observation time series in Fig. 6. The deviations are generally below 1 K back until 1955, although the NOAA-20CR has not assimilated those data. Since at 00:00 GMT most ascents are nighttime ascents, the radiation error in those soundings is likely small. Only before 1955 the deviations are larger, which indicates an inhomogeneity either in the observations (possibly the pressure sensor) or in the NOAA-20CR. From 1958 onwards also ERA-40 background departures are available. These show even smaller variance, partly because upper-air data have been assimilated. Interestingly, the NOAA-20CR and ERA-40 background departures are highly correlated and show synchronous dips such as around 1969, which clearly indicates inhomogeneities in the observations rather than in the analyses/background forecasts. From such a simple comparison one can immediately see the benefit of having different (and largely independent) departure time series at one's disposal. If the same fluctuations are visible in all background departure time series, the likelihood for inhomogeneities in the observations is dramatically increased. The ERA-Interim background departures in Fig. 9 are again smaller than those from ERA-40, most likely due to the substantially improved data assimilation system compared to ERA-40. Of course any detected inhomogeneity raises the desire for proper homogenization of the observation records, as it is undertaken in Ramella Pralungo and Haimberger (2014) at least for wind data.

The global upper-air network time coverage and distribution are presented in Figs. 2 and 1. In order to explore the development of the global upper-air network, it is interesting to examine, decade by decade, the number and the positions of the operative stations. In Fig. 10 the development

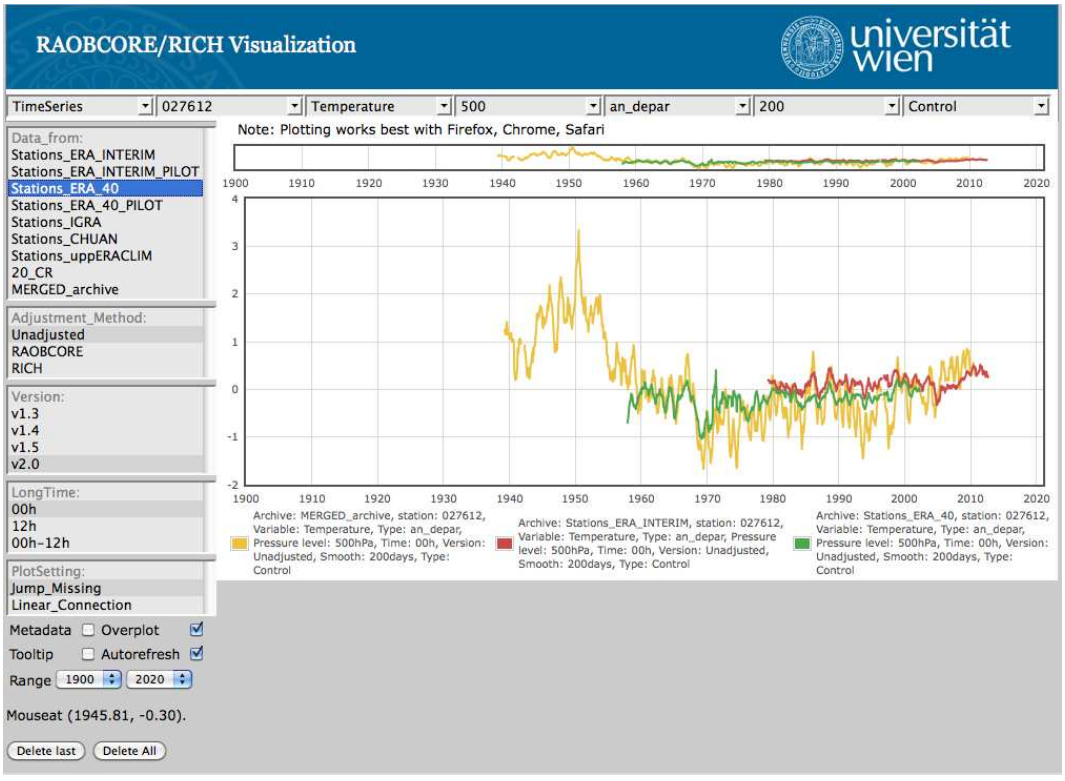


**Figure 9.** Time series of 500 hPa, 00:00 GMT departures between observations at Moscow and reference data sets derived from reanalysis efforts: obs-NOAA 20CR analysis (yellow); obs-ERA-40 (green) 6 h background forecasts, obs-ERA-Interim 12 h background forecasts (red).

of the upper-air observing network is displayed, where only stations with more than 5 years of observations for the selected decade have been plotted. The first systematic wind observations are dated 1920 over the United States, and they become denser from 1935 onward. In the years 1945/1950 in Europe, Russia (even if in Moscow temperature observations have been maintained since 1938), and Japan, a rudimentary upper-air observation network was present. In Australia, New Zealand, Hawaii, Polynesia, and Africa, a very small number of stations was active. Also stationary weather ships were operative in the Atlantic and Pacific oceans. The global coverage becomes satisfactory already in the decade 1950–1960 in the Northern Hemisphere. Good spatial coverage has been maintained over the whole globe, but observations remain scarce over central Africa and South America.

The global radiosonde network reached its maximum extent, in terms of number of stations, in 1957/58, during the International Geophysical Year with more than 1600 active stations (roughly 1200 reported wind and 900 reported temperature). In December 2012, 825 stations were active: 713 reported temperature and 804 reported wind.

Table 2 summarizes how the single archives contribute to the merged archive. For temperature ECUD and CHUAN data, 66.3 and 45.1 %, respectively, of the available observations have been ingested in the merged archive. The percentages are not higher because the most recent data stored in these archives are partly overlapping with IGRA and/or ERA-40, and those have higher data priority. For wind, more than 70 % of the ECUD and CHUAN data flow into the merged archive. The newly digitized and compiled (ECUD and CHUAN) data contribute roughly 4.8 % (temperature) and 10.4 % (wind) to the merged archive.

After the merging procedure, 37 station records contain more than 70 years of continuous observations, which makes them extremely interesting and valuable for further studies. When analysing those data, one has to be aware of the changing quality of the observations. The nominal precision of temperature measurements is $\pm 0.2$ K (GCOS, 2007), but the actual precision is likely less, especially for the earlier measurements, which used relatively thick, slowly responding sensors. In addition, the precision of the pressure measurements as well as of the interpolation procedure has to be taken into account. Thus it is not surprising that Wartenburger et al. (2013) found much larger observation errors on the order of 1 K for soundings in the 1940s and 1950s. Only for the modern GPS-based sounding systems, the nominal precision is actually reached. While the actual increase of precision with time depends on the radiosonde type used as well as on the altitude of the measurements, it is very likely not better than $\pm 0.5$ K in the 1980s, as can be seen also from

**Table 2.** Data contribution of different archives to the merged archive. The order of data sets is also the order of preference when merging. Thus the 66.3 % of data used from ECUD are data found only in ECUD.

| | Temperature | | | | |
|---|---|---|---|---|---|
| | ERA-Int | ERA-40 | IGRA | CHUAN | ECUD |
| % data used | 99.9 | 48.5 | 13.8 | 45.1 | 66.30 |
| % data respect total | 52.4 | 32.8 | 10.0 | 4.7 | 0.1 |
| | **Wind** | | | | |
| | ERA-Int | ERA-40 | IGRA | CHUAN | ECUD |
| % data used | 99.9 | 53.7 | 13.9 | 78.8 | 70.4 |
| % data respect total | 48.2 | 32.7 | 8.8 | 9.7 | 0.7 |

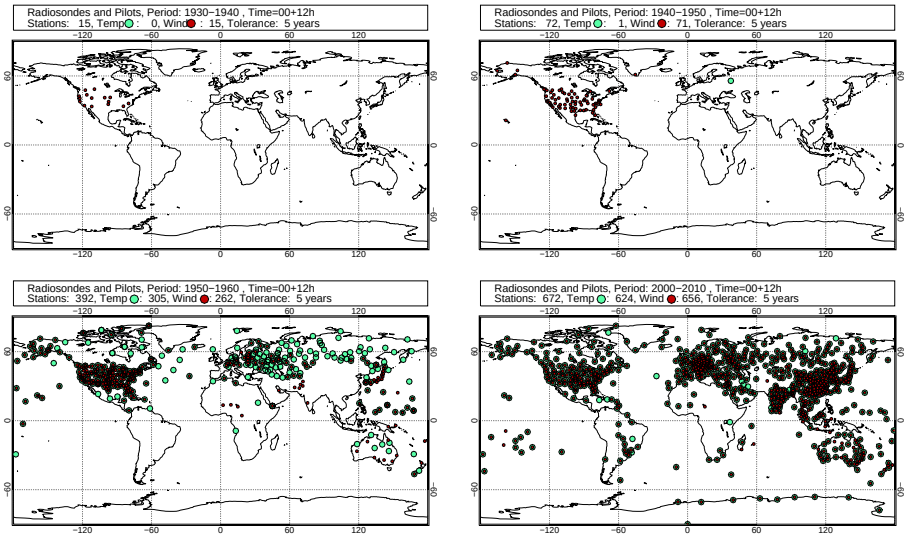


**Figure 10.** Decadal distribution of upper-air stations in the merged archive with at least 5 years of data in the range 850–500 hPa, starting 1930–1940 (upper left) to 2000–2010 (bottom right). Only WMO stations have been used.

the early radiosonde intercomparison experiments (Nash and Schmidlin, 1987). The time series of background departures can also serve as an upper bound for the precision of the measurements, although their variance is determined not only by measurement precision but also by representativeness errors and the quality of the analyses or background forecasts used. Figure 9 shows how the background departures have decreased over time. Regarding measurement accuracy (also called trueness or bias), the quality depends even more on radiosonde type for temperature. Biases larger than 1 K above 100 hPa are common for many radiosonde types still used in the 1990s (Haimberger et al., 2008). One should keep that in mind when using the merged data, which are given with four decimal places ($10^{-4}$ K) to be able to trace them back to the original measurements (often given in °C or °F).

Regarding wind data, the situation is similar. Not only measurement reliability but also precision has improved when switching from theodolites to RADAR and then further to GPS-based soundings. It is nowadays of the order of 1 m s$^{-1}$ for wind speed and 5° for wind direction with a vertical resolution of 200 m (GCOS, 2007). When using theodolites, the precision was worse, but not more than a factor of 2, as can be seen from time series of background departures of wind in the 1940s and 1950s (see Ramella Pralungo and Haimberger, 2014). Nevertheless, the numbers in the netCDF files have not been rounded to ensure clean conversion of units (kt, km h$^{-1}$ to m s$^{-1}$).

## 8 The time-series viewer

For simple time-series visualization, a JavaScript-based time-series viewer, (available at the page http://srvx7.img.univie.ac.at/~lorenzo/DEVL_rrvis_2.0/html/) was developed. It allows quick monitoring of the data archive, which permits visual detection of outliers and shifts. One can choose between observed variables (temperature and wind speed, direction, $U$ and $V$ components) and departures from different background series (NOAA 20CR, ERA-Interim and ERA-40). Observation time (00:00, 12:00 and 00:00–12:00 UTC difference) and the pressure level can be

selected from the self-explanatory menu. More details about the viewer can be found at http://reanalyses.org/observations/raobcorerich-visualization.

## 9 Conclusions

The presented merged data set contains upper-air temperature and wind records on standard pressure levels back to the 1920s. It is specifically targeted for advanced quality control and bias adjustments and, of course, climatological analysis. It complements existing upper-air data sets (ECUD, CHUAN, IGRA, ERA-40 input, ERA-Interim input) that are in total perhaps more complete (they contain altitude and/or pressure levels and also short time series with less than 300 days with observations) but also more difficult to use and not always aligned as time series. It contains not only the raw observations but also departures from the NOAA 20th century reanalysis and ERA-40/ERA-Interim background forecasts. As such the data set is particularly suitable as a basis for a homogenized temperature and wind data set that uses RAOBCORE (Haimberger, 2007) technology for bias adjustments. The homogeneity adjustments for wind and their effect on the time series and global mean trends are described in part 2 of this paper (Ramella Pralungo and Haimberger, 2014). The archive is available in convenient NetCDF format and can be visualized with a simple online plotting tool. The archive will be updated once a year shortly after a full year has been completed in ERA-Interim.

The altitude to standard pressure level conversion involved the use of NOAA 20CR geopotential information. The time resolution is relatively coarse, and future surface-pressure-only reanalyses, such as ERA-20C (Poli et al., 2013), will help to improve this aspect since the upper-air data have been passively assimilated at the correct time which consequently yields background departures at the right time. Future surface-data-only reanalyses also may have smaller temperature and wind biases than the NOAA-20CR.

## Appendix A: NetCDF file structure

All input data archives as well as the merged archive have been written as NetCDF files that contain the time series with daily resolution (00:00 and 12:00 UTC ascents) at 16 standard pressure levels (10, 20, 30, 50, 70, 100, 150, 200, 250, 300, 400, 500, 700, 850, 925 and 1000 hPa). One file is written for each variable (temperature, $U$ wind and $V$ wind components) and station.

The file names are self-explanatory:

123456_V_$t$.$nc$. (A1)

The first digit is either 0 or 1:

- 0 indicates that the station has been identified as a WMO station.
- 1 indicates that the station has been identified as a NO WMO station.

The next five digits are the WMO station identification number, if the first is a 0; otherwise they are the progressive number with which the station has been saved in the respective archive (CHUAN or ECUD, since only those two archives contain unknown stations). The $V$ refers to the variable reported in the file, and it can be

- $T$ ⟶ temperature
- $U$ ⟶ $U$ wind component
- $V$ ⟶ $V$ wind component.

The _t refers to time series, as is the form in which the data have been stored. In the file are defined 13 dimensions, 18 variables and the global attributes. The variable list is composed of (type ⟶ name)

- integer ⟶ stations ⟶ station ID, it works as the first six digits in the file name (according to A1)
- float ⟶ lat ⟶ station latitude, in degrees north, range $[-90°, 90°]$
- float ⟶ long ⟶ station longitude, in degrees east, range $[-180°, 180°]$
- float ⟶ alt ⟶ station altitude, in in m a.s.l., range $[-400, 8000]$ m
- integer ⟶ pressure_layers(16) ⟶ array with the 16 standard pressure levels
- integer ⟶ obs_time(2) ⟶ array with launch times (00:00 and 12:00) UTC
- integer ⟶ date(45000) ⟶ progressive day index from 1900-01-01 with Gregorian calendar, range [19000101, 20230316]
- integer Varno ⟶ the variable number identifier following the ECMWF line guides (Upper Air Temperature 2 [K]; $U$ component of wind 3 [m s$^{-1}$]; $V$ component of wind 4 [m s$^{-1}$])
- integer ⟶ index_days ⟶ progressive (from 1). Date(index_days) returns the corresponding day that refers to index_days for the selected station.
- float ⟶ obs ⟶ The observations array could be named, in agreement with the variable reported in the file name:
  - Temperature ⟶ temperature
  - U_Wind ⟶ $U$ wind component
  - V_Wind ⟶ $V$ wind component

  The arrays have dimensions obs(obs_time, pressure_layers, index_days) In this way, we use the minimum number of days in order to map the time series.

After the observed time series, the departure (background departures from ERA-Interim, ERA-40 and analysis departures from NOAA 20CR) flags and measurement system type information are stored as follows:

- float ⟶ bias correct ⟶ bias correct(obs_time, pressure_layers, index_days), only available for ERA-Interim and ERA-40 archives, where bias correction procedure has been performed by ECMWF (Haimberger and Andrae, 2011; Andrae et al., 2004);
- float ⟶ fg_depar ⟶ fg_depar(obs_time, pressure_layers, index_days), only available for ERA-Interim and ERA-40 archives, where it has been performed as Observation-Forecast first guess (ECMWF forecast);
- float ⟶ an_depar ⟶ an_depar(obs_time, pressure_layers, index_days), for ERA-Interim and ERA-40 archives it has been performed as Observation-Analysis (ERA-40 or ERA-Interim Reanalysis ECMWF ); for IGRA, CHUAN, ECUD and merged archive, the analysis comes from NOAA 20CR fields (updated to 2010);
- integer ⟶ sonde_type ⟶sonde_type(index_days) contains information about the WMO measurement system type (see http://www.wmo.int/pages/prog/www/IMOP/meetings/Upper-Air/Radiosonde-netw/Doc5-3.pdf)
- integer ⟶ status ⟶ status(obs_time, pressure_layers, index_days) contains the data source archive for the current obs_time, pressure_layers, index_days:

  - status=1 ⟶ ERA-Interim input
  - status=2 ⟶ ERA-40 input
  - status=3 ⟶ IGRA archive
  - status=4 ⟶ CHUAN archive
  - status=5 ⟶ ECUD.
- integer ⟶ anflag anflag(obs_time, pressure_layers, index_days) flag, reserved for future use;
- integer ⟶ event1 event1(obs_time, pressure_layers, index_days) flag, reserved for future use.

The file is equipped with global attributes:

- conventions = “CF-1.4” ⟶ NetCDF files conventions
- title ⟶ project title
- institution ⟶ file owner "University of Vienna"
- history ⟶ when the file was produced
- data type ⟶ “RADIOSONDE INPUT DATA”
- source ⟶ source archive
- references: ⟶ www.univie.ac.at/theoret-met/research/raobcore.

Routines for reading the archived NetCDF files are available in FORTRAN and IDL and can be downloaded from doi:10.1594/PANGAEA.823609.

**Acknowledgements.** This work has been funded by projects P21772-N22 and P25260-N29 of the Austrian Fonds zur Förderung der wissenschaftlichen Forschung (FWF), as well as by the EU 7th Framework Programme collaborative project ERA-CLIM (grant no. 265229) and by the Swiss National Science Foundation (project EVALUATE). The authors thank the collaborators within ERA-CLIM, most notably Hans Hersbach and Alexander Sterin for their support and constructive comments.

Edited by: G. König-Langlo

## References

Adam, W. K. and Dier, H.: Lange Messreihen zur Wetter- und Klimaforschung am Meteorologischen Observatorium Lindenberg, ProMet, 31, 159–170, 2005.

Allan, R., Brohan, P., Compo, G. P., Stone, R., Luterbacher, J., and Brönnimann, S.: The international atmospheric circulation reconstructions over the earth (ACRE) initiative, B. Am. Meteorol. Soc., 92, 1421–1425, doi:10.1175/2011BAMS3218.1, 2011.

Andrae, U., Sokka, N., and Onogi, K.: The radiosonde temperature bias correction in ERA-40, Volume 15 of ERA-40 Project Report Series, ECMWF, 2004.

Blunden, J. and Arndt, D. S.: State of the climate in 2012, B. Am. Meteorol. Soc., 94, S1–S258, doi:10.1175/2013BAMSStateoftheClimate.1, 2013.

Brönnimann, S.: A historical upper air-data set for the 1939–44 period, Int. J. Climatol., 23, 769–791, 2003.

Brönnimann, S. and Luterbacher, J.: Reconstructing northern hemisphere upper-level fields during World War II, Clim. Dynam., 22, 499–510, doi:10.1007/s00382-004-0391-3, 2004.

Brönnimann, S., Stickler, A., Griesser, T., Ewen, T., Grant, A. N., Fischer, A. M., Schraner, M., . Peter, T., Rozanov, E., and Ross, T.: Exceptional atmospheric circulation during the "Dust Bowl", Geophys. Res. Lett., 36, L08802, doi:10.1029/2009GL037612, 2009.

Brönnimann, S., Grant, A. N., Compo, G. P., Ewen, T., Griesser, T., Fischer, A. M., Schraner, M., and Stickler, A.: A multi-data set comparison of the vertical structure of temperature variability and change over the arctic during the past 100 years, Clim. Dynam., 39, 1577–1598, doi:10.1007/s00382-012-1291-6, 2012.

Compo, G. P., Whitaker, J. S., Sardeshmukh, P. D., Matsui, N., Allan, R. J., Yin, X., Gleason, B. E., Vose, R. S., Rutledge, G., Bessemoulin, P., Brönnimann, S., Brunet, M., Crouthamel, R. I., Grant, A. N., Groisman, P. Y., Jones, P. D., Kruk, M. C., Kruger, A. C., Marshall, G. J., Maugeri, M., Mok, H. Y., Nordli, Ã., Ross, T. F., Trigo, R. M., Wang, X. L., Woodruff, S. D., and Worley, S. J.: The twentieth century reanalysis project, Q. J. Roy. Meteor. Soc., 137, 1–28, doi:10.1002/qj.776, 2011.

Compo, G. P., Whitaker, J. S., Sardeshmukh, P. D., and Giese, B.: Developing the sparse input reanalysis for climate applications (SIRCA) 1850–2014, http://conference2011.wcrp-climate.org/orals/B4/Compo_B4.pdf (last access: 12 May 2014), WMO, 2012.

Dee, D. P., Uppala, S. M., Simmons, A. J., Berrisford, P., Poli, P., Kobayashi, S., Andrae, U., Balmaseda, M. A., Balsamo, G., Bauer, P., Bechtold, P., Beljaars, A. C. M., van de Berg, L., Bidlot, J., Bormann, N., Delsol, C., Dragani, R., Fuentes, M., Geer, A. J., Haimberger, L., Healy, S. B., Hersbach, H., Hólm, E. V., Isaksen, L., Kallberg, P., Köhler, M., Matricardi, M., McNally, A. P., Monge-Sanz, B. M., Morcrette, J. J., Park, B. K., Peubey, C., de Rosnay, P., Tavolato, C., Thépaut, J. N., and Vitart, F.: The ERA-Interim reanalysis: configuration and performance of the data assimilation system, Q. J. Roy. Meteor. Soc., 137, 553–597, doi:10.1002/qj.828, 2011.

Durre, I., R. Vose, and D.B. Wuertz, 2006: Overview of the Integrated Global Radiosonde Archive. J. Climate, 19, 53–68.

Free, M., Seidel, D. J., Angell, J. K., Lanzante, J., Durre, I., and Peterson, T. C.: Radiosonde atmospheric temperature products for assessing climate (RATPAC): A new data set of large-area anomaly time series, J. Geophys. Res., 110, D22101, doi:10.1029/2005JD006169, 2005.

GCOS, 2008: GCOS Reference Upper-Air Network (GRUAN): Justification, requirements, siting and instrumentation options. Technical document 1379, WMO, 2007.

Grant, A., Brönnimann, S., Ewen, T., and Nagurny, A.: A new look at radiosonde data prior to 1958, J. Climate, 22, 3232–3247, 2009.

Gruber, C. and Haimberger, L.: On the homogeneity of radiosonde wind time series. Meteorol. Z., 17, 631–643, 2008.

Haimberger, L.: Homogenization of radiosonde temperature time series using innovation statistics, J. Climate, 20, 1377–1403, 2007.

Haimberger, L. and Andrae, U.: Radiosonde temperature bias correction in ERA-Interim, ERA report series, 8, http://old.ecmwf.int/publications/library/ecpublications/_pdf/era/era_report_series/RS_8.pdf (last access: 19 May 2014), 2011.

Haimberger, L., Tavolato, C., and Sperka, S.: Towards elimination of the warm bias in historic radiosonde temperature records – some new results from a comprehensive intercomparison of upper air data, J. Climate, 21, 4587–4606, 2008.

Haimberger, L., Tavolato, C., and Sperka, S.: Homogenization of the global radiosonde temperature dataset through combined comparison with reanalysis background series and neighboring stations, J. Climate, 25, 8108–8131, 2012.

Jourdain, S. and Roucaute, E.: Historical upper air data rescue at meteo-france for ERA-CLIM, in: EMS Annual Meeting Abstracts, Volume 10, http://meetingorganizer.copernicus.org/EMS2013/EMS2013-97.pdf (last access: 12 May 2014), 2013.

Nash, J. and Schmidlin, F. J.: WMO International Radiosonde Intercomparison: Final Report, WMO/TD No. 195, WMO, Geneva, 1987.

Poli, P., Hersbach, H., Tan, D., Dee, D., Thepaut, J. N., Simmons, A., Peubey, C., Laloyaux, P., Komori, T., Berrisford, P., Dragani, R., Tremolet, Y., Holm, E., Bonavita, M., Isaksen, L., and Fisher, M.: The data assimilation system and initial performance evaluation of the ECMWF pilot reanalysis of the 20th-century assimilating surface observations only (ERA-20C), ECMWF, 2013.

Ramella Pralungo, L. and Haimberger, L.: A global radiosonde and tracked balloon archive on 16 pressure levels (GRASP) back to 1905 – Part 2: Homogeneity adjustments for PILOT and radiosonde wind data, Earth Syst. Sci. Data Discuss., 7, 335–383, doi:10.5194/essdd-7-335-2014, 2014.

Redder, C. R., Luers, J. K., and Eskridge, R. E.: Unexplained discontinuity in the U.S. radiosonde temperature data. part II: Stratosphere, J. Atmos. Ocean. Tech., 21, 1133–1144, 2004.

Seidel, D. J., Berger, F. H., Immler, F., Sommer, M., Vömel, H., Diamond, H. J., Dykema, J., Goodrich, D., Murray, W., Peterson, T., Sisterson, D., Thorne, P., and Wang, J.: Reference upper-air observations for climate: Rationale, progress, and plans, B. Am. Meteor. Soc., 90, 361–369, 2009.

Sherwood, S. C., Meyer, C. L., Allen, R. J., and Titchner, H. A.: Robust tropospheric warming as revealed by iteratively homogenized radiosonde data, J. Climate, 21, 5336–5352, 2008.

Stickler, A. and Brönnimann, S.: Significant bias of the ncep/ncar and twentieth century reanalyses relative to pilot balloon observations over the west african monsoon region (1940–57), Q. J. Roy. Meteor. Soc., 137, 1400–1416, doi:10.1002/qj.854, 2011.

Stickler, A., Grant, A. N., Ewen, T., Ross, T. F., Vose, R. S., Comeaux, J., Bessemoulin, P., Jylhä, K., Adam, W. K., Jeannet, P., Nagurny, A., Sterin, A. M., Allan, R., Compo, G. P., Griesser, T., and Brönnimann, S.: The comprehensive historical upper air network (CHUAN), B. Am. Meteor. Soc., 91, 741–751, doi:10.1175/2009BAMS2852.1, 2010.

Stickler, A., Brönnimann, S., Jourdain, S., Roucaute, E., Sterin, A., Nikolaev, D., Valente, M. A., Wartenburger, R., Hersbach, H., Ramella-Pralungo, L., and Dee, D.: Description of the ERA-CLIM historical upper-air data, Earth Syst. Sci. Data, 6, 29–48, doi:10.5194/essd-6-29-2014, 2014.

Thorne, P. W., Parker, D. E., Tett, S. F. B., Jones, P. D., McCarthy, M., Coleman, H., and Brohan, P.: Revisiting radiosonde upper-air temperatures from 1958 to 2002, J. Geophys. Res., 110, D18105, doi:10.1029/2004JD005753, 2005.

Thorne, P. W., Brohan, P., Titchner, H. A., McCarthy, M. P., Sherwood, S. C., Peterson, T. C., Haimberger, L., Parker, D. E., Tett, S. F. B., Santer, B. D., Fereday, D. R., and Kennedy, J. J.: A quantification of uncertainties in historical tropical tropospheric temperature trends from radiosondes, J. Geophys. Res., 116, D12116, doi:10.1029/2010JD015487, 2011.

Uppala, S.M., P.W. Kållberg, A.J. Simmons, U. Andrae, V. da Costa Bechtold, M. Fiorino, Gibson, J. K., Haseler, J., Hernandez, A., Kelly, G. A., Li, X., Onogi, K., Saarinen, S., Sokka, N., Allan, R. P., Andersson, E., Arpe, K., Balmaseda, M. A., Beljaars, A. C. M., van de Berg, L., Bidlot, J., Bormann, N., Caires, S., Chevallier, F., Dethof, A., Dragosavac, M., Fisher, M., Fuentes, M., Hagemann, S., Hólm, E., Hoskins, B. J., Isaksen, L., Janssen, P. A. E. M., Jenne, R., McNally, A. P., Mahfouf, J. F., Morcrette, J. J., Rayner, N. A., Saunders, R. W., Simon, P., Sterl, A., Trenberth, K., Untch, A., Vasiljevic, D., Viterbo, P., and Woollen, J.: The ERA-40 Re-analysis, Q. J. Roy. Meteor. Soc., 131, 2961–3012, 2005.

Wartenburger, R., Brönnimann, S., and Stickler, A.: Observation errors in early historical upper-air observations. J. Geophys. Res., 118, 12012–12028, doi:10.1002/2013JD020156, 2013.